

## Strontium Doping Concentrations Influence on $\text{La}_{1-x}\text{Sr}_x\text{MnO}_{3-\delta}$ Micro Structural and Electrical Conductivity

B. S. Kamble<sup>1</sup>, V.J. Fulari<sup>2</sup>, R. K. Nimat<sup>3</sup>.

<sup>1</sup>Department of Physics, D.B.J.College, Chiplun-415605,India.

<sup>2</sup>Department of Physics, Shivaji University, Kolhapur-416004,India

<sup>3</sup>Department of Physics, Balasaheb Desai College, Patan-415206,India.

**Abstract:** Different types of ceramic materials are currently being studied as possible cathodes in solid oxide fuel cell(SOFC),due to reduce operating temperatures. Strontium doped lanthanum manganite ( $\text{La}_{1-x}\text{Sr}_x\text{MnO}_{3-\delta}$ -LSM) was used as cathode for solid oxide fuel cell (SOFC). LSM thin film with 0.1, 0.2 and 0.3 mol % strontium were synthesized by spray pyrolysis technique. The thin films were sintered at  $800^\circ\text{C}$  has been characterized by Infra-red spectroscopy, X-ray diffraction to determine the crystalline perovskite phase, Scanning electron microscopy and FESEM are used for morphological analysis. D.C.electrical conductivity was measured with variation of temperature and it increases due to increase of Sr content. Dielectric constant was measured with frequency variation. Thermal conductivity and specific heat was measured at atmospheric temperature.

**Keywords:** Spray Pyrolysis, Electrical conductivity, Dielectric constant, Cathode, LSM, SOFC.

### I. Introduction

Recently solid oxide fuel cells (SOFC) are used as energy conversion devices with high efficiency, modularity and low pollution [1-5]. Strontium doped lanthanum manganite ( $\text{La}_{1-x}\text{Sr}_x\text{MnO}_{3-\delta}$ -LSM) is considered as a classic material for SOFC on account of its good electronic conductivity, thermal, mechanical stability [6-8]. Reduction of operating temperature to  $600-700^\circ\text{C}$  is now the primarily hurdle for commercialization of SOFC [9]. Many research groups have synthesized LSM material as cathode in bulk form. Synthesis of SOFC materials in the thin film form will help to reduce the cost and operating temperature of SOFC. We have synthesized the LSM material in the thin form by spray pyrolysis technique.

Strontium is preferential element chosen for the attainment of high electronic conductivity, because it increases of  $\text{Mn}^{+4}$  ions formation and the substitution of  $\text{La}^{3+}$  for  $\text{Sr}^{2+}$  [10].

This work presents a variation of Sr concentration to the study of structural and electrical properties of  $\text{La}_{1-x}\text{Sr}_x\text{MnO}_{3-\delta}$  by spray pyrolysis technique. The film has been characterized by X-ray Diffractometry (XRD), Infrared spectroscopy and Scanning electron microscopy (SEM). The electrical properties were studied.

### II. Experimental

Prior to deposition, the precursor solution of Lanthanum Nitrate hex hydrate ( $\text{La}(\text{NO}_3)_3 \cdot 6\text{H}_2\text{O}$  Loba Chmie), Strontium Nitrate ( $\text{Sr}(\text{NO}_3)_2$  Loba chime) and Manganese Nitrate hex hydrate ( $\text{Mn}(\text{NO}_3)_3 \cdot 6\text{H}_2\text{O}$ -ALFA ASER) are dissolved in double distilled water, formed precursor used for sprayed using glass nozzle with spray rate  $3\text{ml}/\text{min}$  on alumina substrates placed on hot plate and at  $250^\circ\text{C}$ , this leads to pyrolytic decomposition of these metallic salts and formation of Lanthanum Strontium Manganite thin film as per the doping concentration maintained in precursor that means we can also control the doping concentration of Strontium. The crystallization of material was achieved by annealing at  $800^\circ\text{C}$  for 2 hours.

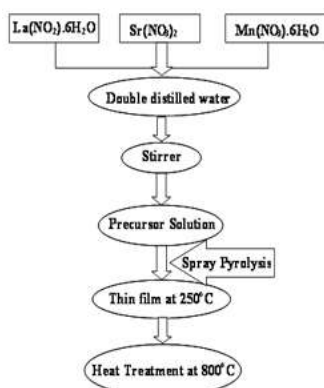


Fig. 1 The systematic flow-chart of spray pyrolysis technique

The sintered films were then characterized for their structural and morphological properties. The structural properties of the film were determined using X-ray diffractometer (PHILIPS PW-3710) with Cu K $\alpha$  radiation source. Morphological characteristics were analyzed using Scanning Electron Microscope (SEM, JEOL- SSM-6360). The Infra-red spectrum was recorded by using Perkin Elmer infra-red spectrophotometer with scanning range 500-4000  $\text{cm}^{-1}$ . D.C. conductivity of prepared  $\text{La}_{1-x}\text{Sr}_x\text{MnO}_{3-\delta}$  film was measured by two probe method using lab made resistivity set up in air. Dielectric constant was measured by HEWLETT 4284A PACKARD 20Hz-1MHz LCR meter and thermal conductivity was measured by C.T. meter at atmospheric temperature.

### III. Results And Discussion

#### 3.1 Film formation:

Fig.1 shows schematic flow-chart of spray pyrolysis technique. The deposition of thin film via spray pyrolysis involves spraying a metallic salt solution on a heated substrate. The solution droplets reach the substrate surface, where solvent evaporation and decomposition of the metal salt occurs, forming a film. Many processes occur sequentially or simultaneously during the formation of thin film by spray pyrolysis i.e. transport and evaporation of solution drops, solution spread on the substrate, evaporation of solvent. This includes aerosol. The drops of solution are transported and eventually evaporate. Except aerosol all processes are temperature dependent<sup>[11]</sup>. The substrate temperature and solution concentration are main parameters responsible to affect the thickness and morphology of the thin films. It needs to optimize the LSM thin film. A good morphology and uniform thin film is reported at 0.05M concentration. So solution concentration was varied from 0.01 M to 0.1 M keeping the substrate temperature fixed at 250°

#### 3.2 XRD studies:

Fig.4. displays the XRD pattern of the LSM thin film sintered at 800°C for 2 hours. XRD result indicates the formation of LSM perovskite structure, according to PCPDF (WIN) file 047-0444. The lattice parameter decreases with increasing  $\text{Sr}^{2+}$  content<sup>[12]</sup>. The observed in XRD study confirms trigonal crystal with space group  $R\bar{3}c$ . The unit cell is rhombohedral with hexagonal lattice parameter. This result shows that thin solid films are polycrystalline.

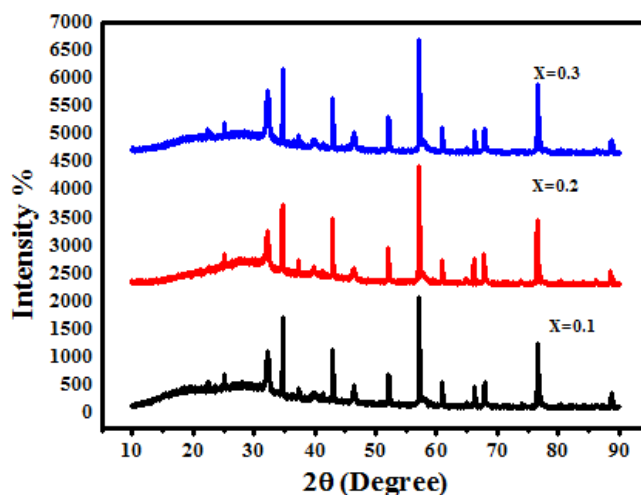


Fig.4) The XRD of LSM thin films sintered at 800°C

#### 3.3 Scanning electron micrograph and FESEM:

The morphological study of LSM thin film is made by JEOL Scanning Electron Microscope shows porous morphology. The porosity composed due to crystallites of Lanthanum Strontium Manganite<sup>[13]</sup>. The SEM images show porous morphology which is applicable as cathode for solid oxide fuel cell as it is necessary in order to pass oxygen ions at cathode-electrolyte interface<sup>[14]</sup>. The micro structure of  $\text{La}_{0.9}\text{Sr}_{0.1}\text{MnO}_{3-d}$  thin films heat treated at 800°C for  $x = 0.1, 0.2, 0.3$  were investigated as a function of strontium content<sup>[15]</sup>.

From Fig.7, a less porous microstructure is observed for high strontium content. Fig.7(c) shows formation of grain boundaries among the small grains. The grain size shows significant modification with the strontium content. The grain size of the  $\text{La}_{1-x}\text{Sr}_x\text{MnO}_{3-\delta}$  film is approximately 200nm and this value decreases with increase Sr content. However, whatever the strontium content, the film thickness is too low for SOFC application. This is because multilayers are synthesized in order to increase film thickness<sup>[16]</sup>.

Fig.8 shows FESEM images of LSM thin film. The nano-thin films were prepared by spray pyrolysis technique have a spongy aspect and a good size distribution and good particle separation.

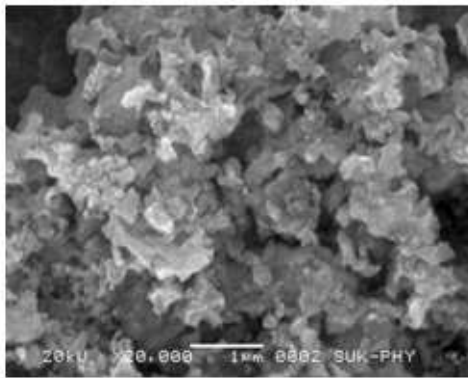


Fig.7 a) The SEM images of LSM thin films  $x=0.1$

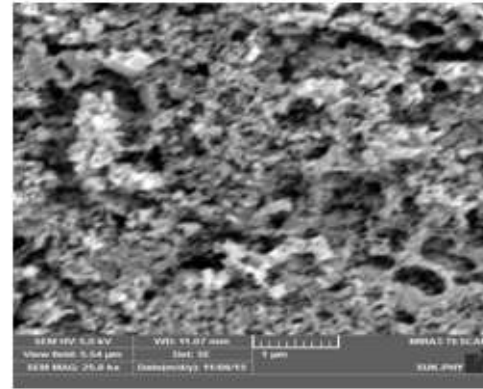


Fig.8 a) The FESEM images of LSM thin films  $x=0.1$

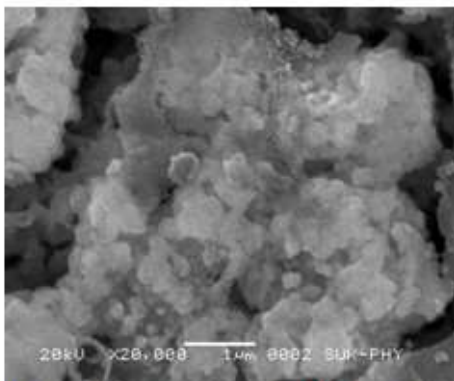


Fig.7 b) The SEM images of LSM thin films  $x=0.2$

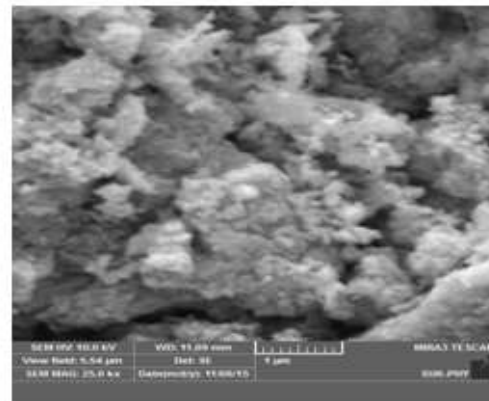


Fig.8 b) The FESEM images of LSM thin films  $x=0.2$

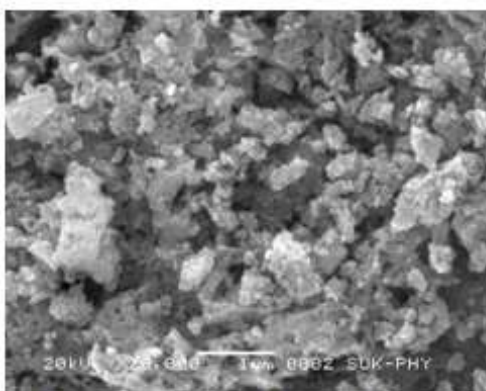


Fig.7 c) The SEM images of LSM thin films  $x=0.3$

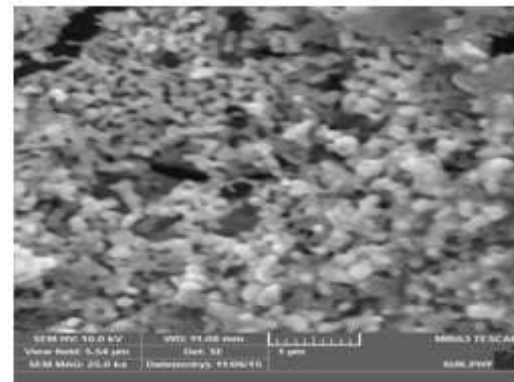


Fig.8 c) The FESEM images of LSM thin films  $x=0.3$

### 3.4 FT-Infrared Study:

The Fourier transforms infrared spectra of the strontium – lanthanum manganite samples are shown in Fig.9. The band at  $450\text{cm}^{-1}$ - $500\text{cm}^{-1}$  is due to the existence of cubic  $La_2O_3$  [17]. The absorption bands present at  $2000\text{cm}^{-1}$ - $2500\text{cm}^{-1}$  are due to some decomposition products of this solvent. The band observed at  $980\text{cm}^{-1}$  -  $1000\text{cm}^{-1}$  was referred to C-O bond [18]. The main absorption band located near  $700\text{cm}^{-1}$  and it is assigned metal-oxide stretching in the perovskite structure [19].

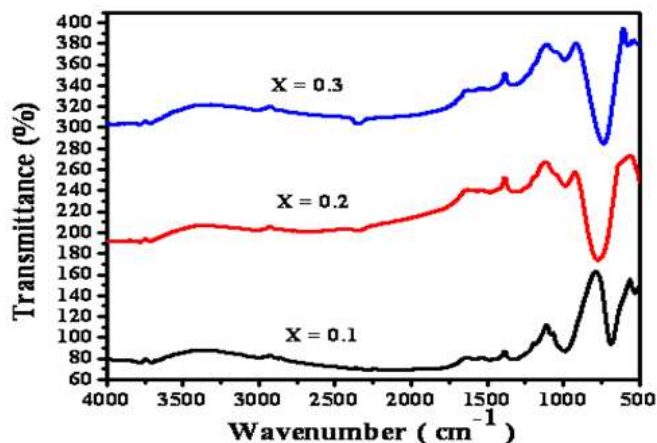


Fig.9 FT-IR Spectra of LSM thin films

### 3.5 D.C. Conductivity:

Strontium doping enhance the electronic conductivity of LSM due to increased  $\text{Mn}^{4+}$  content which results from the substitution of  $\text{La}^{3+}$  by  $\text{Sr}^{2+}$ . The performance of a LSM cathode material of SOFC is influenced by not only the chemical stability and thermodynamic characteristics of LSM of the cathode material but also by its microstructure, grain and pore size distribution.

Fig.10 shows the graph of product of logarithm conductivity and absolute temperature as a function of reciprocal of absolute temperature. The addition of  $\text{Sr}^{2+}$  to  $\text{La}^{3+}$  in A-site causes the changes in oxidation states of Mn ions. The electrical conductivity of LSM is controlled by  $\text{Sr}^{2+}$  substitution for  $\text{La}^{3+}$  [20]. It is well known that the Mn ions can be divalent, trivalent or tetravalent [21]. The Mn ions tend to exist in the form of  $\text{Mn}^{3+}$  in the atmospheric conditions. The  $\text{Sr}^{2+}$  substitution for  $\text{La}^{3+}$  can be consequently compensated by either electron hole ( $\text{h}^{\circ}$ ) or oxygen vacancy ( $\text{Vo}^{\circ\circ}$ ). The Sr substitution for La enhances the electrical conductivity of LSM by increasing the concentration of  $\text{Mn}^{4+}$ , owing to the combination of  $\text{Mn}^{3+}$  and  $\text{h}^{\circ}$  [22].

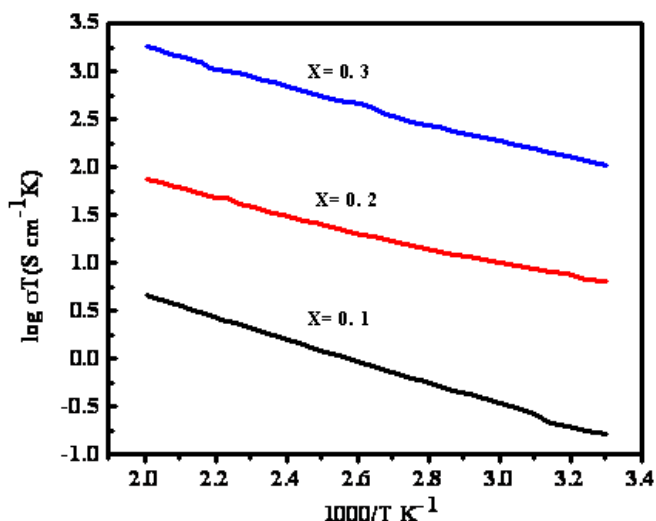
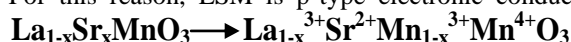


Fig.10. D.C.conductivity of LSM thin films

The substitution of  $\text{La}^{3+}$  increases the content of  $\text{Mn}^{4+}$  in the structure creating electronic holes for keeping charge neutrality. For this reason, LSM is p-type electronic conductor under oxidant atmosphere.



Not only electronic conductivity but also ionic conductivity is present due to the fact that vacancies are introduced for non-stoichiometric oxygen content and aliovalent substitution [23].

### 3.6 Thermal Conductivity:

Thermal conductivity of LSM thin film was carried out by C.T meter at room temperature with heating time 25 sec and measuring time 100 sec. The thermal conductivity of LSM film is shown in Table.1. It is found that as strontium content increases thermal conductivity and specific heat both increases.

composition	Thermal Conductivity (W/mK)	Specific heat (KJ/m <sup>3</sup> K)
x= 0.1	0.191	203
x= 0.2	0.198	227
x= 0.3	0.199	243

Table No.1

### 3.7 Dielectric Constant:

Fig.11. depicts the plot of dielectric constant Vs frequency having compositions  $x = 0.1, 0.2$  and  $0.3$  sintered at  $800^\circ\text{C}$  for 2 hours. At low frequency dielectric constant is very high and as frequency increases dielectric constant decreases and further increasing frequency dielectric constant remain constant.

The higher dielectric constant at lower frequencies is associated with heterogeneous conduction in composites, but sometimes the polaron hopping mechanism results in electronic polarization contributing at low frequency dispersion [24].

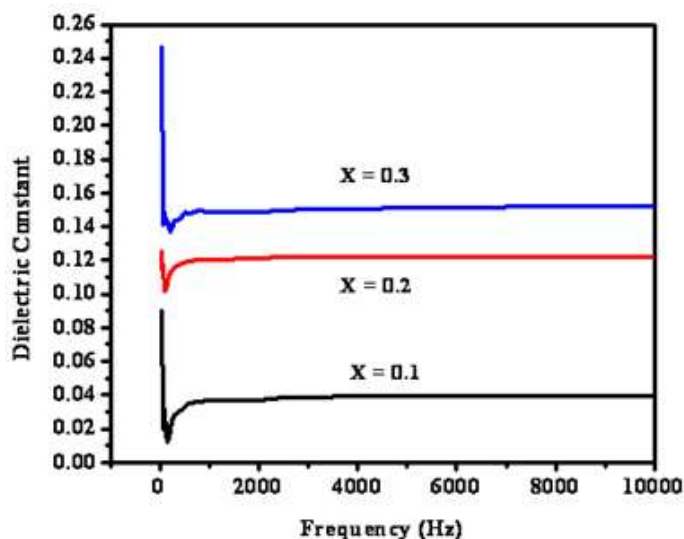


Fig.11. Dielectric constant of LSM thin film

## IV. Conclusion

The performances of LSM cathode synthesized by spray Pyrolysis technique were investigated. The XRD patterns exhibit a perovskite structure. The investigated composition of  $La_{1-x}Sr_xMnO_{3-\delta}$  sintered samples with  $x$  varying from  $x = 0.1$  to  $0.3$  showed polycrystalline film with rhombodendral structure having hexagonal lattice parameter. The LSM thin film sintered at  $800^\circ\text{C}$  are shows homogeneous with porosity. The smooth porous surface is observed by SEM and FESEM. FT-IR spectrum confirms the perovskite structure. Electrical conductivity can be described by small polaron hopping conductivity model and increase with regular increments of Sr content.

## References

- [1]. P.Lenormand, A.Lecomte.C. Leberly, F.Ansart, A.Boulle, J. of Matter.sci.(2009) 42:4581-4590.
- [2]. Dongbo Zhang, Lei Yang, ZE liu, Kenin Blinn, Jae-Wung Lee, Meilin Liu, Applied surface science 258(2012) 6199-6203.
- [3]. Moises R. Cesario,Danial A.Macedo, Rosane M.P. B.Oliveria,Patricia M. Pimental, `Roberto L.Moreira and Dulce M.A.Melo. Journalof Ceramic Processing Research Vol.12, No.1pp.102-105(2011)
- [4]. ZHENG Yingping, GE Shan, ZHOU Xueying, CHEN Hong, HUANG Shuo, WANG Shaorong, SUN Yuming, Journal of Rare Earths. Vol.30 No.12,Dec.2012 p.1240
- [5]. Fei Ye, Zhicheng Wang, Wenjian Weng, Kui Cheng, Chenlu Song, Piyi Du, Ge Shen, Gaorong Han, Thin solid films 516 (2008) 5206-5209.
- [6]. D.J.Babu, A.J.Darbandi, J.Suffner, S. S. Bhattacharya, H. Hann., Transaction of the Indian Institute of Metals., vol.64, Issues 1&2, Feb-Apr.-2011, p-p 181-184.
- [7]. Glauber S. Godoi, Dulica. P. F. de Souza, Materials Science and Engineering B 140 (2007) 90-97
- [8]. Piao Jinhua, Sun Kening, Zhang Naiqing, Xu Shen, Journal of Rare Earths vol.24. spec. Issu. Dec.2006, p-93.
- [9]. V.S.Reddy Channu, Rudolf Holze, Edwin H. Walkar. New Journal of Glass and Ceramics, 2013, 3, 29-33.Moises R. Cesario,Danial A.Macedo, Rosane M.P. B.Oliveria,Patricia M. Young-Hoon Choi, Segoo Kang, Jurgen Wackerl, Kyoung-Tac Lim, Doo-Hwan Jung, Taejin Kim and Dong-Hyun Peck, Journal of Ceramic Processing Research. Vol.14, No.2, pp.153-158 (2013).
- [10]. Vladimir Strbik-Stefan Chromik. Journal of ELECTRICAL ENGINEERING, Vol.62, No.4, 2012, 270-272.
- [11]. Adriano Alberto, Marfran Cardoso de et al.Material Research, 2011; 14(1):91-96.
- [12]. Jitendra Kumar, Rajiv K.singh, P.K.Siwach, H.K.Singh, Ramadhar Singh, R.C. Rastogi, O.N. Srivastava. Solid State communicatios 138 (2006) 422-425.

- [13]. Seo Miyamura, E.S.Couto, A.A; Lima, N.B., Kolher A.C.; PreriaSoares E.
- [14]. D.Perednis, L.J.Gauckler. Solid State Ionics 166(2004) 229-239
- [15]. M.Navseriy, S.A.Halim, G.Bahmanrokh, M.Erfani H. N.Soltani, A. Dehzangi, A. Kamalianfar, F.Ud.Din, S. Abdolmohammadi, S.K.Chen, L.A. Mehdipour and A.Annur. Int. J. Electrochem.Sci., 8 (2013) 6905-6921.
- [16]. M. Gaudon, C. baberty-Robert, F.Ansart, P. Stevens & A.Rousset. Journal of New Materials for electrochemical system 57-61 (2002).
- [17]. Carlos Vazquez-Vazquez, M-Arturo Lopez-Quintela, Journal of solid state chemistry 179 2006) 3229-3237.
- [18]. Ardiano Alves Rabelo, Marfran Cardoso de Macedo, Duice Maria de Araujo Melo, Carlos Alberto Paskocimas, Antonio Eduardo Martinelli, Rubens Maribondo do Nascimento, Materials Research 2011; 14(1): 91-96.
- [19]. N.Q.Minh, Ceramic fuel cells, J.Am. ceram soc 76(3) (1993), 563-588.
- [20]. G.V.Subba Rao, C.N.R.Rao, J.R.Ferraro, Applied spectrosc. 24(1970) 436.
- [21]. S.Fritsch, A. Navrotsky, Thermodynamics properties of manganese oxides, J.Am, Ceram.Soc 79(7) (1996) 1761-1768
- [22]. S.U.Dubal, A.P.Jamale, S.T.Jadhav, S.P.Patil, C.H.Bhosale, L.D.Jadhav. Journal of alloys and compounds 587 (2014) 664-669.
- [23]. Jacqueline C.MARRERO, Nielson F.P. RIBERIO, Celia F. MALEFATTI, Mariana M. V. M. SOUZA, Journal of Advanced Ceramics 2013, 2(1): 55-62
- [24]. J.C.Marrero, N.F.P.Ribero, C.F.Malfatti, M.M.V.m.Souza, Journal of Advanced ceramics 2013, 2(1); 55-62.